

Supporting Information for:

**C–Cl Activation of the Weakly Coordinating Anion [B(3,5–C₆H₃Cl₂)₄][–] at a Rh(I)
Centre in Solution and the Solid–State.**

Sebastian D. Pike and Andrew S. Weller*

Department of Chemistry, Inorganic Chemistry Laboratories, University of Oxford, Oxford, OX1 3QR,
UK.

Experimental	S-2
<i>Synthetic Methods:</i>	
1	S-2
2	S-3
<i>Anti-3</i>	S-4
<i>Syn-3</i>	S-5
4	S-7
5	S-8
6	S-9
Kinetic Plots	S-10
Solid State NMR	S-12
Crystallography	S-13
References	S-17

Experimental Section

General

All procedures, unless otherwise stated were carried out under an argon atmosphere, using standard Schlenk-line and glove box techniques. All glassware was dried at 130°C overnight and flame dried under vacuum before use. Dichloromethane and pentane were dried using a Grubbs type solvent purification system (MBraun SPS-800) and degassed by successive freeze-pump-thaw cycles before use.¹ CD₂Cl₂, chlorobenzene and fluorobenzene were dried over CaH₂, distilled under vacuum and stored over 3 Å molecular sieves. Na[BAr^F₄],² Na[BAr^{Cl}₄],³ were prepared according to literature methods and dried at 120 °C under dynamic vacuum (1 x 10⁻² Torr). [Rh(NBD)Cl]₂, was also prepared by literature methods.⁴ All other chemicals were used as received by the supplier. NMR spectra were recorded on Bruker AVD 500 or a Varian Mercury 300 at room temperature. Chemical shifts quoted in ppm and coupling constants (*J*) quoted in Hz. Residual protio solvent (*e.g.* CD₂Cl₂: δ 5.32 ppm) was used as a reference for ¹H NMR. ESI-MS was carried out upon a Bruker microTOF-Q connected to a glovebox (60°C, 4.5 kV).⁵ ESI Mass spectrometry was attempted only for long lived cationic complexes **1**, **4** and **6**, in the case of dication **6** an ion pair is formed during the experiment with present Br⁻ ions such that the resulting mass is recorded at [M²⁺ + Br⁻]⁺. Elemental micro-analysis carried out upon crystalline samples dried under dynamic vacuum (1 x 10⁻² Torr) overnight, by Stephen Boyer at London Metropolitan University.

Synthetic methods

[Rh(ⁱBu₂PCH₂CH₂PⁱBu₂)(η²η²-C₇H₈)] [BAr^{Cl}₄]**1**.

Prepared as for **A**⁶ except using Na[BAr^{Cl}₄] used instead of Na[BAr^F₄]. Cationic portions of NMR spectra and ESI MS data consistent with **A**.

¹H NMR (300 MHz CD₂Cl₂): δ 1.07 (d (ⁱBu), *J*_{HH} = 6 Hz, 12H), 1.16 (d (ⁱBu), *J*_{HH} = 6 Hz, 12H), 1.62 (m (ⁱBu), 8H), 1.78 (m (PCH₂CH₂P, ⁱBu, NBD), 10H), 4.09 (s (NBD), 2H), 5.31 (s (NBD), 4H), 7.03 (m (BAr^{Cl}₄), 12H)

³¹P {¹H} NMR (122 MHz CD₂Cl₂): δ 48.88 (d, *J*_{RhP} = 155 Hz 2P)

¹¹B {¹H} NMR (160 MHz C₆F₆): δ -6.95 (s, 1B).

ESI MS: ([M⁺] *m/z* = 513.23, [M⁺] calc = 513.23) isotope pattern matches (3 lines)

Elemental Micro-analysis: Calculated for C₄₉H₆₀BP₂Cl₈Rh C, 53.10 H, 5.46 found C, 52.97 H, 5.37. A solid state structure was also recorded (see crystallography section)

Rh(ⁱBu₂PCH₂CH₂PⁱBu₂)((η⁶-C₆H₃Cl₂)BAr^{Cl}₃) 2.

A microcrystalline sample of **1** was exposed to one atmosphere of H₂, either in the solid state or in a CH₂Cl₂ solution, for 30 minutes to give a yellow solid/solution. Relatively rapid recrystallisation from CH₂Cl₂/pentane (277 K, 24 hours) yields yellow crystalline **2** (10 mg (9.0 × 10⁻³ mmol) scale, ~60% yield). (N.B. over time **2** slowly converts to **3** in the solid state, therefore microanalysis was recorded only for **3**).

¹H NMR (500 MHz CD₂Cl₂): δ 0.93 (d, *J*_{HH} = 7 Hz, 12H), 0.98 (d, *J*_{HH} = 7 Hz, 12H), 1.52 (m, 8H), 1.82 (m, ⁱBu CH, PCH₂CH₂P, 8H), 6.15 (s ((BAr^{Cl}₃)C₆H₃Cl₂), 2H), 7.02 (s ((BAr^{Cl}₃)C₆H₃Cl₂), 6H), 7.06 (s ((BAr^{Cl}₃)C₆H₃Cl₂), H), 7.10 (s ((BAr^{Cl}₃)C₆H₃Cl₂), 3H).

³¹P {¹H} NMR (202 MHz CD₂Cl₂): δ 67.84 (d, *J*_{RhP} = 202 Hz, 2P).

¹¹B {¹H} NMR (160 MHz C₆F₆): δ -8.30 (s, 1B).

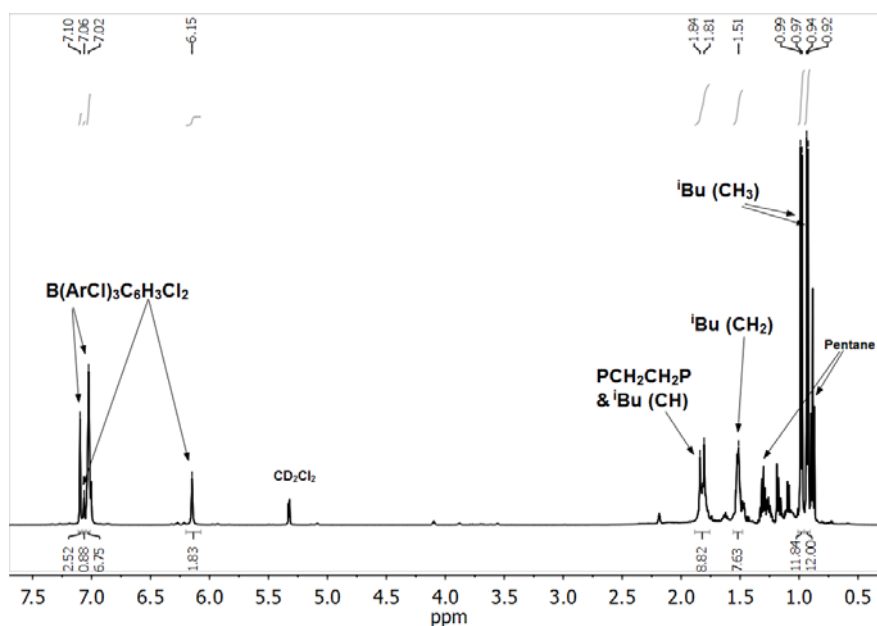


Figure S1. ¹H NMR Spectrum of **2**

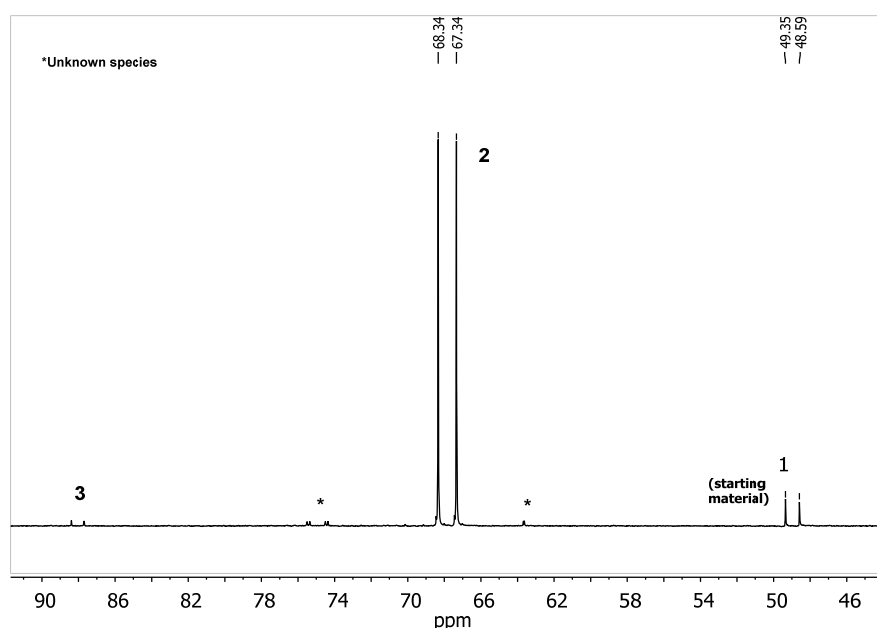


Figure S2. ³¹P {¹H} NMR Spectrum of **2**

[Rh(ⁱBu₂PCH₂CH₂PⁱBu₂)(C₆H₃Cl(BAr^{Cl}₃))Cl]₂ *anti*-3.

Compound **3** forms directly from a CH₂Cl₂ solution of **2** as the *anti* isomer. Crystalline material precipitates directly out of CH₂Cl₂ solutions composed of **3**.(4½ CH₂Cl₂). The complex can also be synthesized using microcrystalline **2** via a solid state route, although a mixture of both *syn* and *anti* isomers forms as the final solid product.

¹H NMR (500 MHz CD₂Cl₂ sparingly soluble): δ 0.72 (d (ⁱBu CH₃), *J*_{HH} = 6 Hz, 12H), 0.89 (d (ⁱBu CH₃), *J*_{HH} = 6 Hz, 12H), 1.08 (d (ⁱBu CH₃), *J*_{HH} = 6 Hz, 12H), 1.13 (d (ⁱBu CH₃), *J*_{HH} = 6 Hz, 12H), 1.6-2.4 (m (iBu & PCH₂CH₂P), 32H, by ¹H COSY analysis ⁱBu CH₂ occur at 1.71 & 2.08), 5.92 (s (C₆H₃Cl(BAr^{Cl}₃)), 2+2H coincidence), 7.00 (s ((C₆H₃Cl(BAr^{Cl}₃)), 12H), 7.08 (s ((C₆H₃Cl(BAr^{Cl}₃)), 6H), 7.11 (s (C₆H₃Cl(BAr^{Cl}₃)), 2H). Small peak at 7.03 ppm is likely to be due to a small amount of non-coordinated [BAr^{Cl}₄], presumably through a small amount of cation decomposition, a small peak is also seen at the appropriate shift for free [BAr^{Cl}₄] in the ¹¹B{¹H} NMR spectrum

³¹P {¹H} NMR (202 MHz CD₂Cl₂): δ 88.00 (d, *J*_{RhP} = 140 Hz, 4P).

¹¹B {¹H} NMR (160 MHz C₆F₆): δ -6.65 (s, 2B).

Elemental Micro-analysis: Calculated for C₈₄H₁₀₄B₂P₄Cl₁₆Rh₂ C, 49.64 H, 5.16 found C, 49.53 H, 5.23

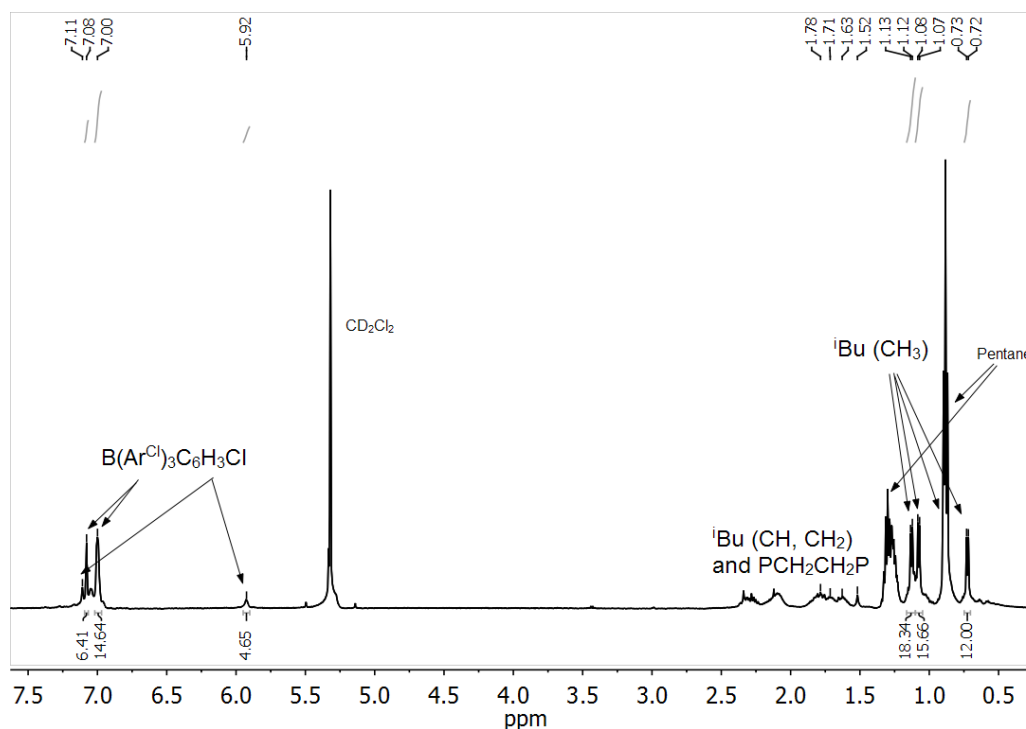


Figure S3. ¹H NMR Spectrum of *anti*-3

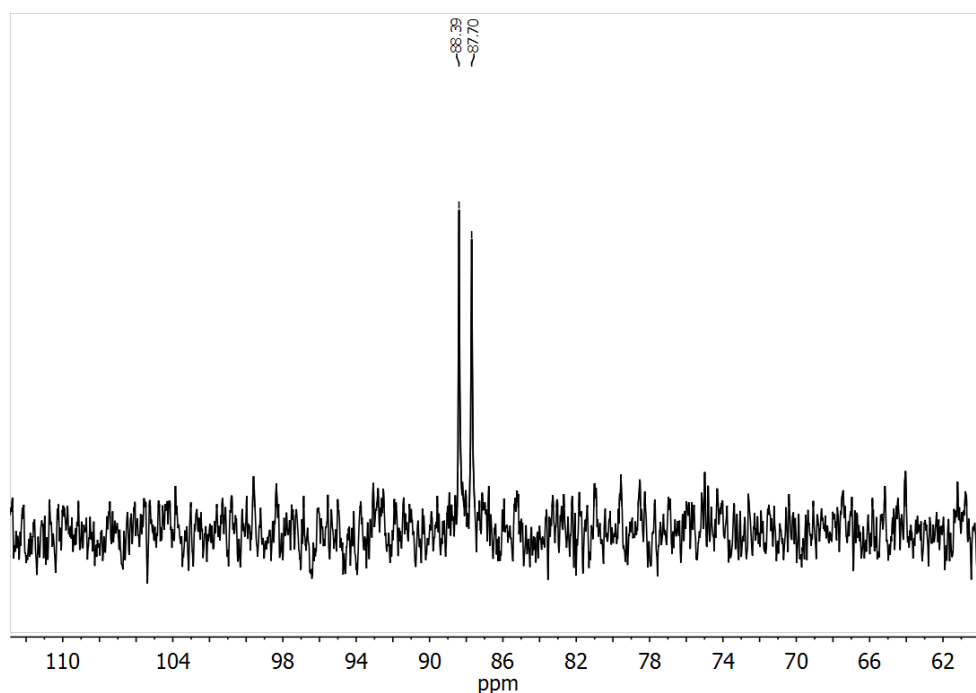


Figure S4. ^{31}P $\{^1\text{H}\}$ NMR Spectrum of *anti*-3

Syn-3 Isomer

Synthesis from **2** in the solid state over 2 weeks, approximately 50% of the product forms as the *syn* isomer.

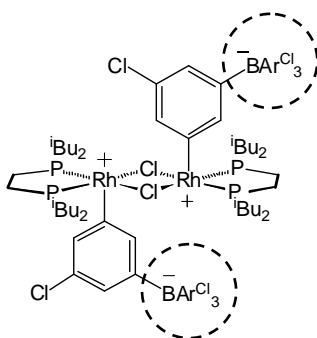


Figure S5. *Syn* isomer of **3** (hindered rotation of Rh-C bond), observed only after solid state synthesis.

NMR spectroscopy data taken from spectra of both isomers mixed (approximately 50% of *syn* isomer)

^1H NMR (500 MHz CD_2Cl_2 sparingly soluble): δ 0.64 (d (^iBu CH_3), $J_{\text{HH}} = 6$ Hz, 6H), 0.72 (d (^iBu CH_3), $J_{\text{HH}} = 6$ Hz, 6H), \sim 0.86 (obscured by pentane (^iBu CH_3), 6H), 0.93 (d (^iBu CH_3), $J_{\text{HH}} = 6$ Hz, 6H), 0.98 (d (^iBu CH_3), $J_{\text{HH}} = 6$ Hz, 6H), 1.10 (d (^iBu CH_3), $J_{\text{HH}} = 6$ Hz, 6H), 1.15 (d (^iBu CH_3), $J_{\text{HH}} = 6$ Hz, 6H), 1.18 (d (^iBu CH_3), $J_{\text{HH}} = 6$ Hz, 6H), 1.4-2.4 (m (^iBu & $\text{PCH}_2\text{CH}_2\text{P}$), 32H), 5.88 (s ($\text{C}_6\text{H}_3\text{Cl}(\text{BAr}^{\text{Cl}}_3)$), 1+1H coincidence), 5.95 (s ($\text{C}_6\text{H}_3\text{Cl}(\text{BAr}^{\text{Cl}}_3)$), 1+1H coincidence), 7.00 (s ($\text{C}_6\text{H}_3\text{Cl}(\text{BAr}^{\text{Cl}}_3)$), 12H), 7.08 (s ($\text{C}_6\text{H}_3\text{Cl}(\text{BAr}^{\text{Cl}}_3)$), 6H), 7.17 (s ($\text{C}_6\text{H}_3\text{Cl}(\text{BAr}^{\text{Cl}}_3)$), 1H), 7.35 (s ($\text{C}_6\text{H}_3\text{Cl}(\text{BAr}^{\text{Cl}}_3)$), 1H)

^{31}P $\{^1\text{H}\}$ NMR (122 MHz CD_2Cl_2): δ 86.88 (d, $J_{\text{RhP}} = 139$ Hz, 2P), 89.09 (d, $J_{\text{RhP}} = 140$ Hz, 2P)

^{11}B $\{^1\text{H}\}$ NMR (160 MHz C_6F_6): δ -6.65 (s, 1B), -6.41 (s, 1B)

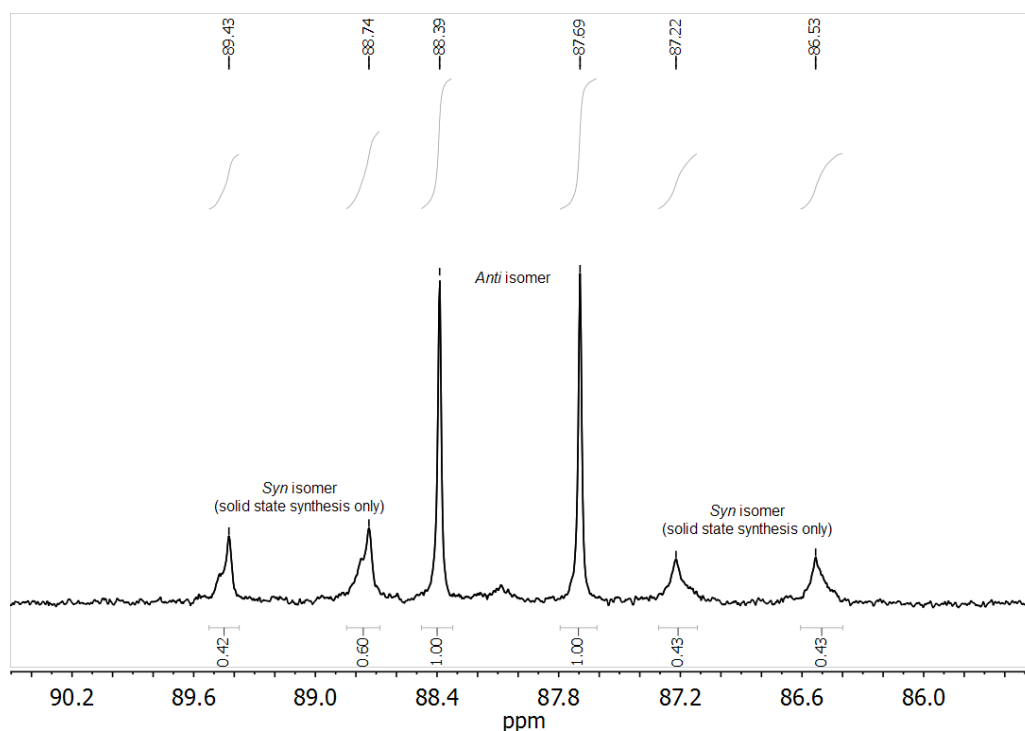


Figure S6. ^{31}P $\{^1\text{H}\}$ NMR spectrum of both isomers together dissolved directly after solid state synthesis (approximately 50% *syn* isomer).

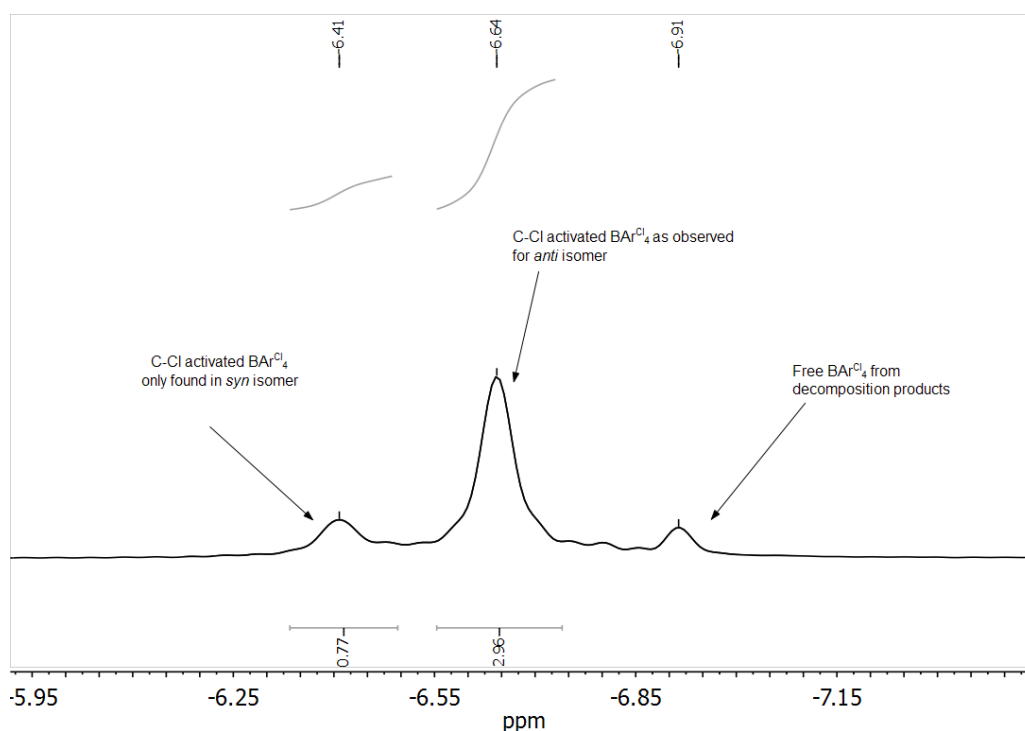


Figure S7. ^{11}B $\{^1\text{H}\}$ NMR spectrum of both isomers together dissolved directly after solid state synthesis (approximately 50% *syn* isomer, we suggest that the *syn* isomer contains one ^{11}B environment coincident with that of the *anti* isomer (6.64 ppm, $\sim 3\text{B}$ total) and one different environment (6.41 ppm, $\sim 1\text{B}$).

Upon heating a mixture of *syn* and *anti* isomers, the ^1H and ^{31}P $\{^1\text{H}\}$ spectra display *anti-3* as the dominant species as *syn-3* converts into the thermodynamic product *anti-3*.

[Rh(ⁱBu₂PCH₂CH₂PⁱBu₂)(η⁶-C₆H₅Cl)][BAR^F₄] 4.

40 mg (0.029 mmol) of [Rh(ⁱBu₂PCH₂CH₂PⁱBu₂)NBD][BAR^F₄] (**A**) was dissolved in a mixture of chlorobenzene (0.5 ml) and CH₂Cl₂ (2 ml) in a Young's flask and this solution exposed to 1 atm H₂. The solution changes to a yellow colour and was left to react for 15 minutes before the tube was degassed. The product was precipitated by adding pentane, with a yield of 64%. The resulting solid can be recrystallised from CH₂Cl₂/pentane.

¹H NMR (500 MHz CD₂Cl₂): δ 1.01 (d, *J*_{HH} = 7 Hz, 12H), 1.09 (d, *J*_{HH} = 7 Hz, 12H), 1.68 (m, 8H), 1.79 (d (PCH₂CH₂P), *J*_{PH} = 17 Hz, 4H), 1.87 (m, 4H), 6.15 (t (C₆H₅Cl), *J*_{HH} = 6 Hz, H), 6.57 (t (C₆H₅F), *J*_{HH} = 6 Hz, 2H), 6.75 (d (C₆H₅F), *J*_{HH} = 6 Hz, 2H), 7.52 (s (BAR^F₄), 4H), 7.72 (s (BAR^F₄), 8H).

³¹P {¹H} NMR (202 MHz C₆H₅F): δ 73.24 (d, *J*_{RhP} = 201 Hz, 2P). ESI MS: ([M⁺] *m/z* = 533.17, [M⁺] calc = 533.17).

Elemental Micro-analysis: Calculated for C₅₆H₅₇BClF₂₄P₂Rh C, 48.14 H, 4.11 found C, 48.08 H, 4.14

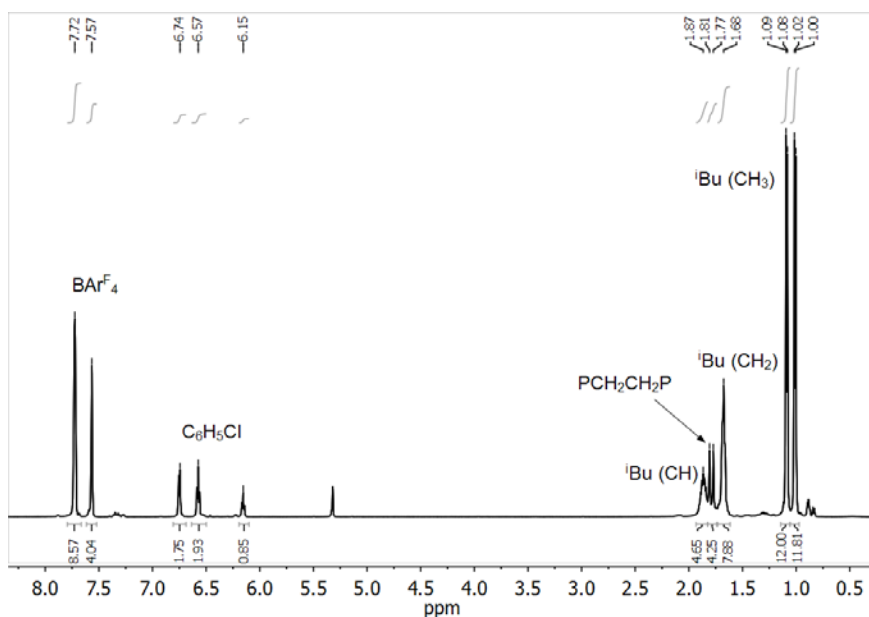


Figure S8. ¹H NMR Spectrum of **4**

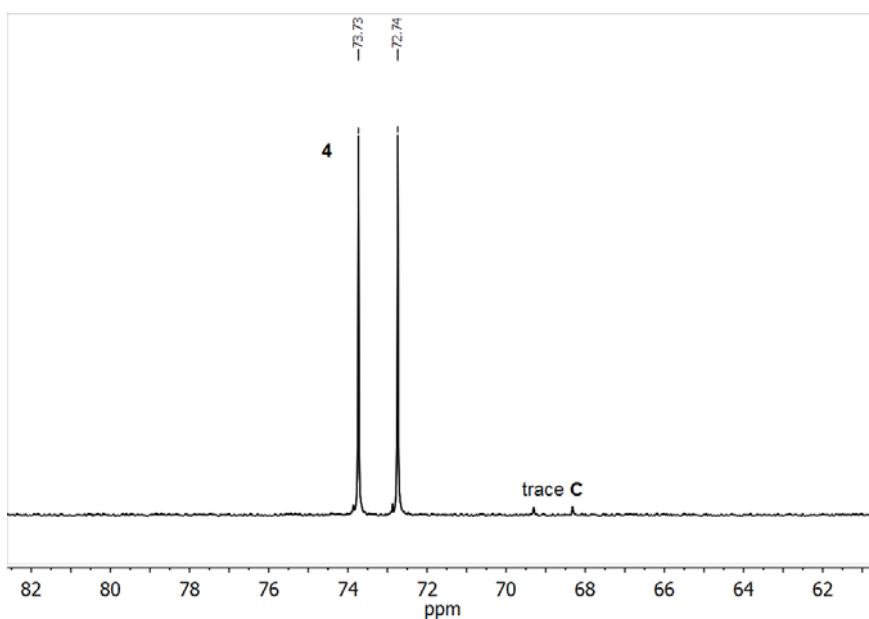


Figure S9. ³¹P {¹H} NMR Spectrum of **4**

[Rh(ⁱBu₂PCH₂CH₂PⁱBu₂)(η⁶-C₆H₅Br)][BAR^F₄] **5.**

15 mg (0.011 mmol) [Rh(ⁱBu₂PCH₂CH₂PⁱBu₂)NBD][BAR^F₄] (**A**) was dissolved in CH₂Cl₂ in a high pressure NMR tube and 10 equivalents of bromobenzene (11.5 μl, 0.11 mmol) added. The tube was charged with 1 atm H₂. A yellow solution forms. **5** rapidly converts into **6**, due to its short lifetime (*t*_{1/2} = 9 min 28 sec) a clean ¹H NMR spectrum free of **5** was not recorded.

³¹P {¹H} NMR (202 MHz C₆H₅F): δ 73.19 (d, *J*_{RhP} = 201 Hz, 2P)

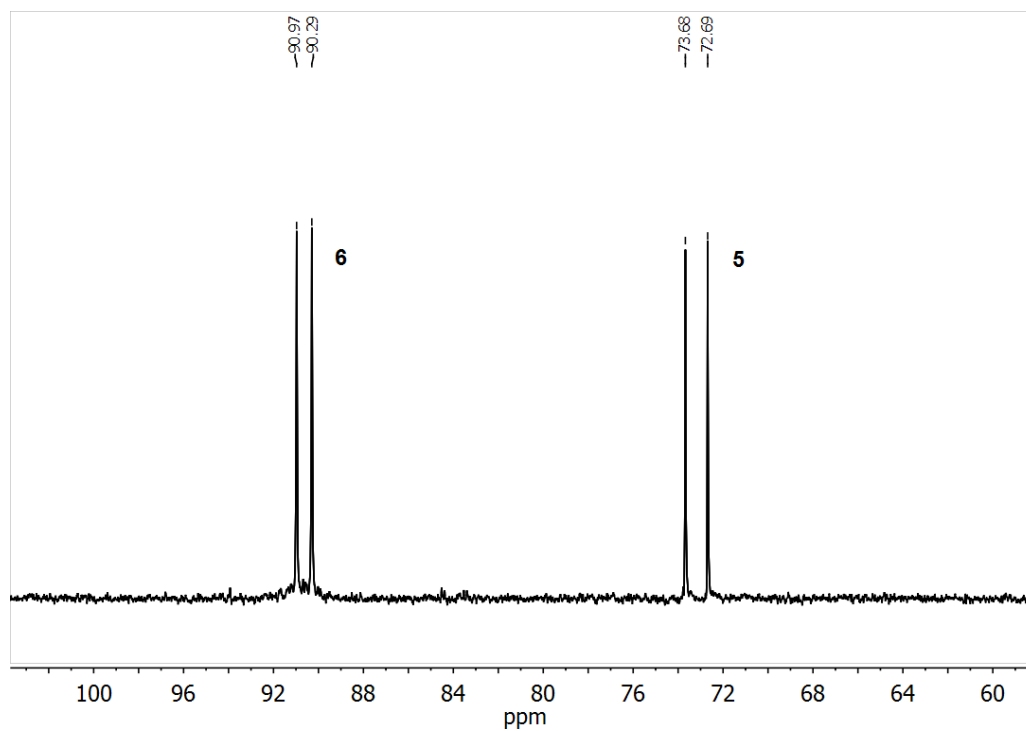


Figure S10. ³¹P {¹H} NMR spectrum during conversion of **5** to form **6**.

[Rh(ⁱBu₂PCH₂CH₂PⁱBu₂)(C₆H₅)Br]₂[BAR^F₄]₂ **6.**

A CH₂Cl₂ solution of **5** (see above) forms **6** directly, after 5 hours pentane was added to precipitate the product and the solid recrystallised in CH₂Cl₂/pentane.

¹H NMR (500 MHz CD₂Cl₂): δ 0.73 (d (ⁱBu CH₃), *J*_{HH} = 6 Hz, 12H), 0.94 (d (ⁱBu CH₃), *J*_{HH} = 6 Hz, 12H), 1.07 (d (ⁱBu CH₃), *J*_{HH} = 6 Hz, 12H), 1.15 (d (ⁱBu CH₃), *J*_{HH} = 6 Hz, 12H), 1.75 (m (ⁱBu CH), 4H), 1.82 (m (ⁱBu CH₂), 4H), 2.02 (m (ⁱBu CH₂), 4H), 2.13 (m (ⁱBu CH), 4H), 2.20 (m (ⁱBu CH₂), 4H), 2.44 (m (ⁱBu CH₂ & PCH₂CH₂P), 12H), 7.07 (m (C₆H₅), 8H), 7.17 (t (C₆H₅), *J*_{HH} = 6 Hz, 2H), 7.57 (s (BAR^F₄), 8H), 7.72 (s (BAR^F₄), 16H).

³¹P {¹H} NMR (202 MHz C₆H₅F): δ 91.78 (d, *J*_{RhP} = 137 Hz, 4P)

ESI MS: ([M²⁺ + Br⁻]⁺ m/z = 1237.12, [M²⁺ + Br⁻] calc = 1237.16).

Elemental Micro-analysis: Calculated for C₁₁₂H₁₁₄B₂Br₂F₄₈O₂P₄Rh₂ C, 46.66 H, 3.99 found C, 46.58 H, 4.06

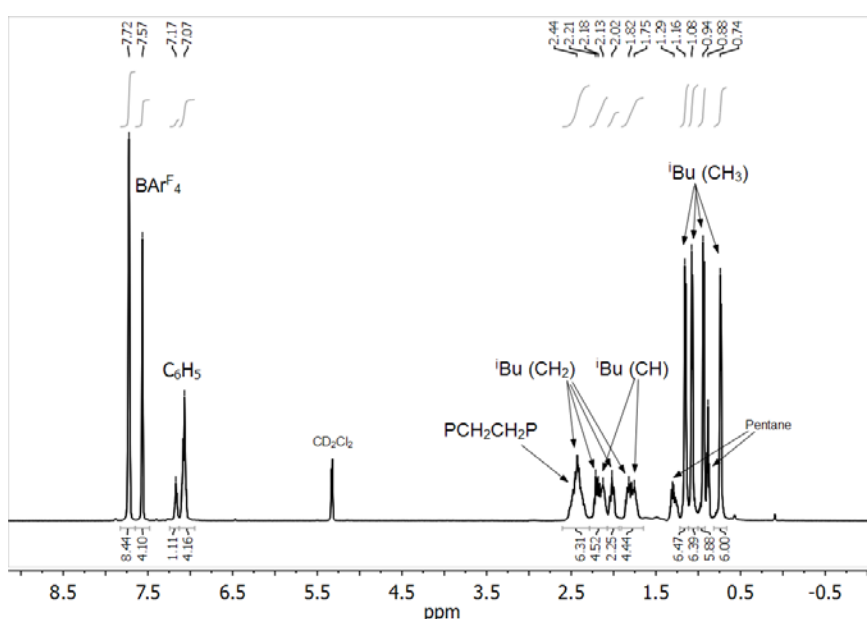


Figure S11. ¹H NMR Spectrum of **6**

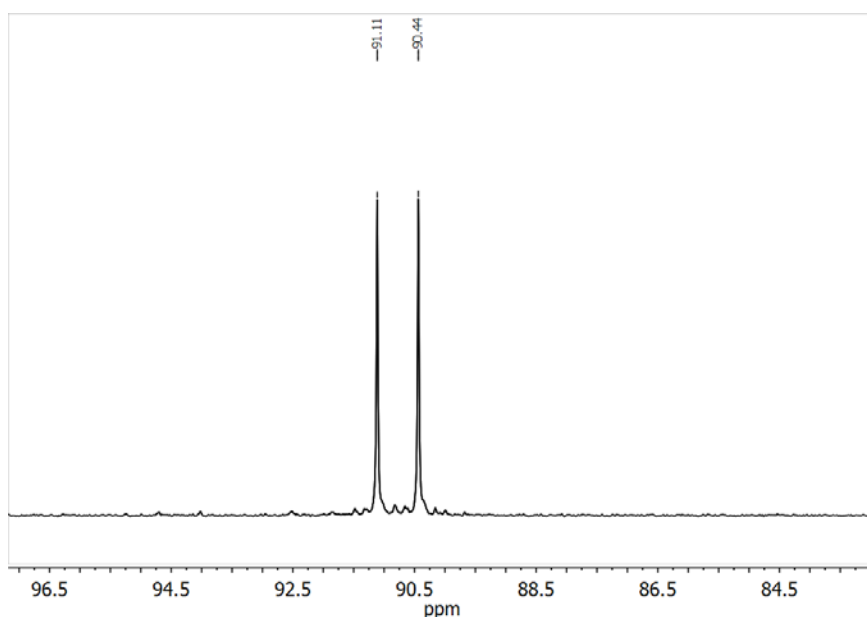


Figure S12. ³¹P {¹H} NMR Spectrum of **6**

Kinetic Plots

Conversion of **2** to **3** in solution

Kinetic experiments were monitored by ^{31}P $\{^1\text{H}\}$ NMR spectroscopy, integration of the signals corresponding to the starting complex **2** was recorded and plotted against time. An NMR insert containing a constant concentration of PPh_3 was used as a standard so that the change in concentration of **2** could be accurately measured (the product **3** precipitates from solution).

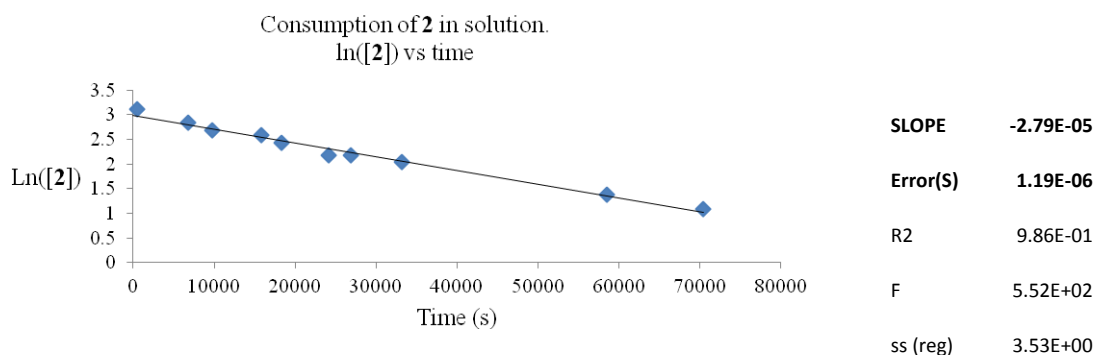


Figure S13. $k_{\text{solution}} = (2.8 \pm 0.1) \times 10^{-5} \text{ s}^{-1}$

Conversion of **2** to **3** in the solid state

Separate microcrystalline samples of **2** were prepared together and kept at room temperature as they converted to form **3** over time. Each was dissolved after a certain duration and the relative ratio of **2** to **3** recorded by integration of the ^{31}P $\{^1\text{H}\}$ NMR spectra, from this the consumption of **2** was plotted. This assumes that no precipitation occurs upon solvation of the solid compounds; the solutions appeared to be homogeneous on formation which suggests precipitation of **3** requires combination with CH_2Cl_2 and occurs slowly in solution. However if precipitation artificially decreases the concentration of **3** then the proportion of **2** will be greater than the true amount resulting in the generation of a rate constant lower than that of the true value.

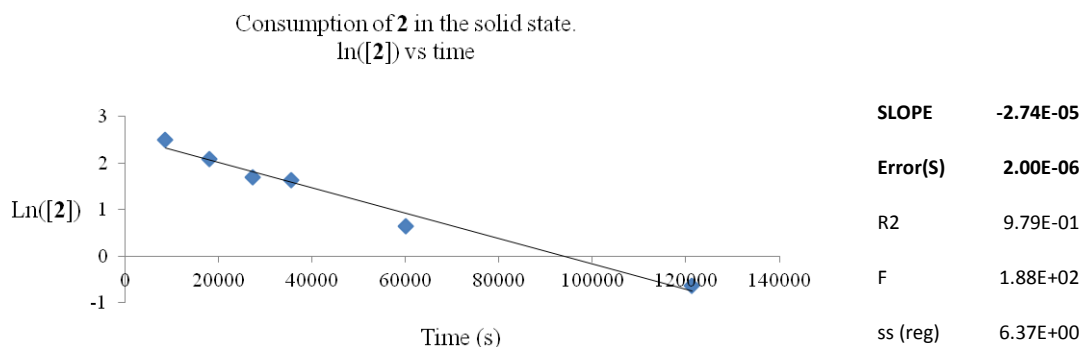


Figure S14. $k_{\text{solid-state}} = (2.7 \pm 0.2) \times 10^{-5} \text{ s}^{-1}$

Conversion of **5** to **6** in solution.

The conversion of **5** to **6** was rapid and was monitored by the consumption of **5** as a percentage of the total ^{31}P $\{^1\text{H}\}$ NMR signal. No precipitation of product was observed as the $[\text{BAr}^{\text{F}}_4]$ anion generally forms more soluble complexes than for those of $[\text{BAr}^{\text{Cl}}_4]$.⁷

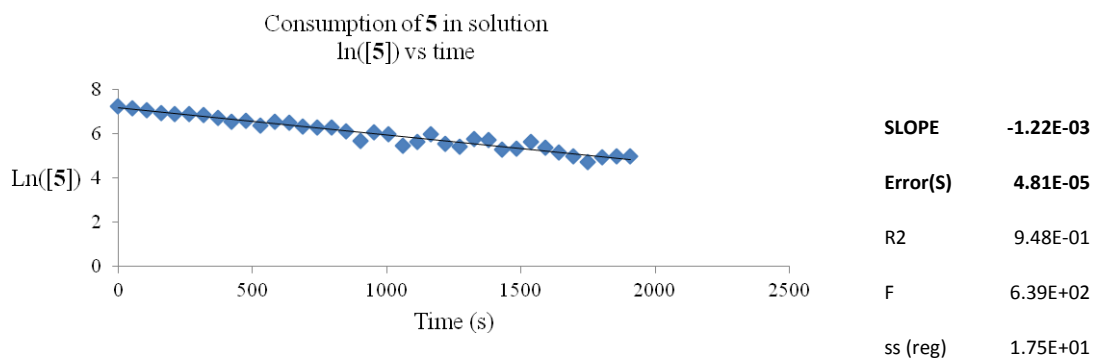


Figure S15. $k_{\text{solution}} = (1.22 \pm 0.05) \times 10^{-3} \text{ s}^{-1}$

Solid State NMR Spectroscopy

Solid-state NMR spectra were recorded at the EPSRC National Solid-State NMR service centre (Durham University) on a Varian VNMRS 400 MHz spectrometer, using the cross-polarization pulse sequence (contact time 3 ms and recycle delay 2 s), with TPPM decoupling. Cross-polarisation experiments were employed in order to avoid the long relaxation delays associated with direct excitation. A spinning rate of 10 kHz was employed. Experiments were undertaken at temperatures from 253 K to 323 K. Spectral referencing is with respect to external neat 85% H₃PO₄ for ³¹P. Spinning was carried out using dry nitrogen. Powdered microcrystalline material was used which had been ground by the back of a spatula thoroughly before use. The sample was loaded into a 4 mm rotor in a N₂ filled glovebox. A pure sample of **1** was analysed by SSNMR initially. In order to undertake the hydrogenation reaction the filled rotor was exposed to one atmosphere of hydrogen with one end left open, using normal Schlenk line apparatus, and the rotor then capped within the glovebox (after evacuation of hydrogen gas).

A sample of **1** was exposed to H₂ (1 atm, 23°C, for 4.5 minutes) to yield a ³¹P {¹H} SSNMR spectrum of **2** (formed as an amorphous material by the solid state reaction) along with a small amount of residual starting material. The sample was then heated stepwise to 323 K. At 323 K the broad peak of **2** begins to convert into another broad peak corresponding to **3** (also in an amorphous form). This process was followed overnight and appears to approach completion within 3 hours. The final product was emptied from the rotor within the glovebox and dissolved in CD₂Cl₂ in order to record solution NMR spectra. These spectra show the expected approximate 1:1 ratio of *syn* and *anti* isomers of **3** and a small amount of residual **1**. This suggests the products of the accelerated reaction at 323 K in the solid state are the same as those generated slowly at ambient temperatures also by solid state reaction.

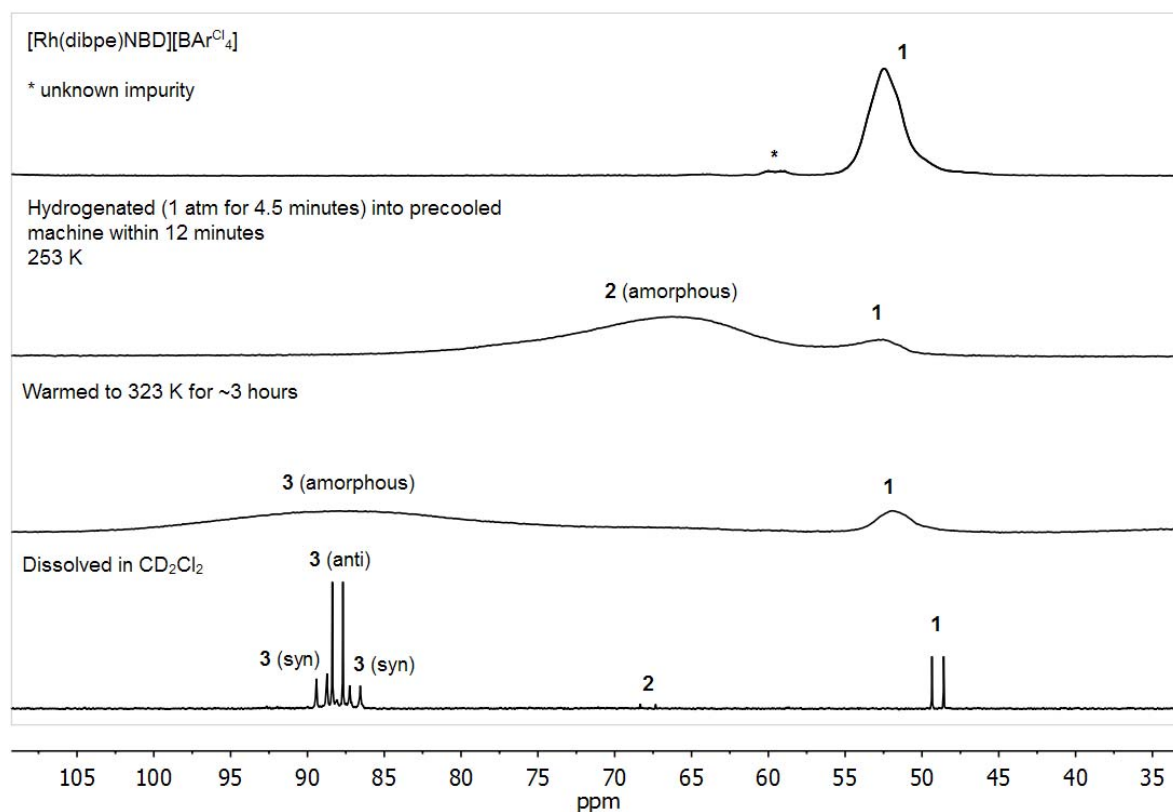


Figure S4. ³¹P {¹H} solid state NMR and solution NMR spectra of **1** and the products of its reaction with hydrogen (first at 253 K and then once warmed to 323 K for 3 hours, final solution spectra at ambient temperature).

Crystallography

X-ray crystallography data for **1** and **6** were collected on an Enraf Nonius Kappa CCD diffractometer using graphite monochromated Mo K α radiation ($\lambda = 0.71073 \text{ \AA}$) and a low-temperature device [150(2) K];⁸ data were collected using COLLECT, reduction and cell refinement was performed using DENZO/SCALEPACK.⁹ The structure was solved by direct methods using SIR2004¹⁰ and refined full-matrix least squares on F^2 using CRYSTALS (**1** and **6**).¹¹ X-ray crystallography data for **2** and **3** were collected on an Agilent SuperNova diffractometer using graphite monochromated Cu K α radiation ($\lambda = 1.54180 \text{ \AA}$) and a low-temperature device [150(2) K];⁸ data were collected using SuperNova, reduction and cell refinement was performed using CrysAlis.¹² The structure was solved by direct methods using Superflip¹³ and refined full-matrix least squares on F^2 using CRYSTALS.¹¹ All non-hydrogen atoms were refined with anisotropic displacement parameters. All hydrogen atoms were placed in calculated positions using the riding model. Crystallographic data have been deposited with the Cambridge Crystallographic Data Centre under **CCDC** 945334-945337. These data can be obtained free of charge from The Cambridge Crystallographic Data Centre via www.ccdc.cam.ac.uk/data_request/cif.

Special details

Compound 1. [Figure S5]

Orange crystals were grown from CH₂Cl₂/Pentane. On initial refinement, the atoms upon one half of the diphosphine fragment exhibited prolate ellipsoids. Examination of the difference Fourier suggested this was due to disorder. Shift limiting restraints were added to aid refinement. One phosphorous atom, its isobutyl substituents and the CH₂CH₂ bridging atoms were modelled over two sites and the disordered isobutyl substituents were restrained to maintain sensible geometries. The disordered PCH₂CH₂P atoms were also separately restrained to maintain sensible geometries. Both disordered groups refined to similar occupancies. The anion was well ordered. The structure and packing is similar to that of **A**.⁶

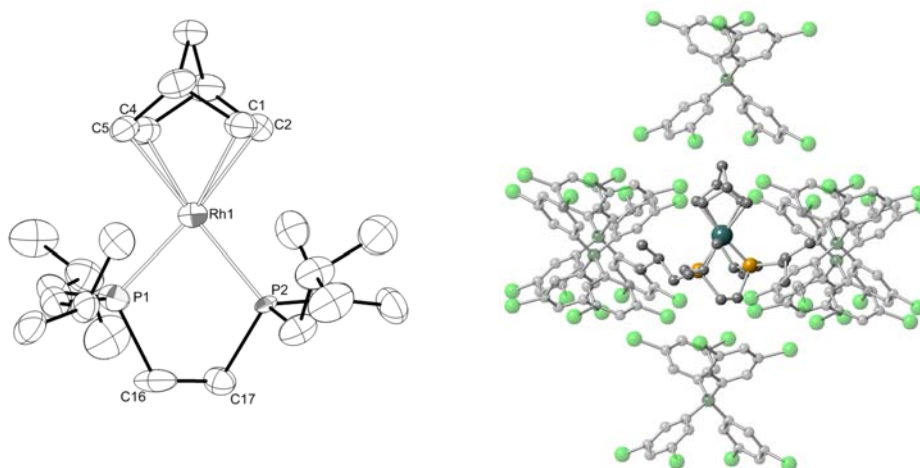


Figure S5. (*left*) Displacement ellipsoid plot (30% probability) for the major cationic component of complex **1** in the solid state. Hydrogen atoms omitted for clarity. (*right*) Crystal packing diagram of **1** showing anions forming a pseudo-octahedron around the cation (anions represented as semi-transparent for clarity, hydrogen atoms omitted).

Compound 2.

Yellow crystals were grown relatively quickly from CH₂Cl₂/Pentane. Disorder of one of the isobutyl substituents was treated by modelling the appropriate isobutyl atoms over two sites and restraining their geometry.

Compound 3.

Yellow crystals were grown directly from CH₂Cl₂ solutions of **2** over several days. The crystals were very delicate and collapsed when removed from the solvent, this is attributed to the high amount of CH₂Cl₂ located in the structure. Unsuccessful X-ray diffraction experiments were attempted upon many of these fractured crystals before a more intact crystal was located which led to a good dataset. The CH₂Cl₂ present in the structure was disordered and some molecules refined to occupancies less than unity. All molecules were restrained to each other to maintain sensible geometries. Two molecules were modelled over two sites (one molecule is disordered across a symmetry plane). A final disordered solvent molecule could not be adequately modelled and so was treated using the SQUEEZE algorithm.^{14, 15}

Compound 4.

The X-ray diffraction pattern of **4** was collected and the space group was determined as C2/c, it appears that a large amount of disorder is present within the structure especially in the phosphine unit which is disordered fairly equally over two positions. Whilst the expected bond connectivity is consistent with the structure, the solution was not of publication quality.

Compound 6. [Figure S6]

Yellow crystals were grown from $\text{CH}_2\text{Cl}_2/\text{pentane}$. Rotational disorder of the CF_3 groups of the anion was treated by modelling the Fluorine atoms over two sites and restraining their geometry. Vibration restraints were used upon the disordered CH_2Cl_2 solvent molecules and they were treated separately. The occupancy of the CH_2Cl_2 molecules were allowed to refine resulting in an occupancies of less than 1, presumably due to partial evaporation of solvent from the crystal. The second molecule was disordered over two sites pivoting about one chlorine atom and was restrained to maintain sensible geometries, the atomic displacement parameters of the carbon atoms in each site were set to ride with each other.

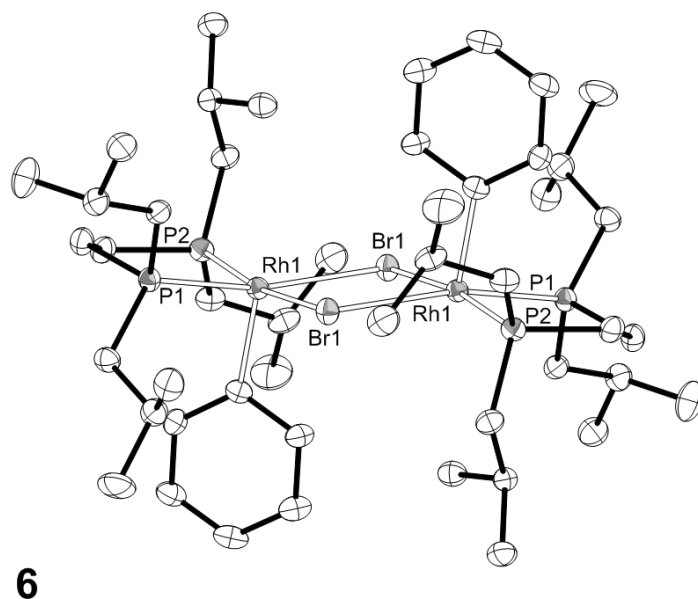


Figure S6. Displacement ellipsoid plot (30% probability) of complex **6** in the solid state. Hydrogen atoms omitted for clarity. Selected Bond (\AA) Data: **6**: Rh1–C1, 2.024(6); Rh1–Br1, 2.5979(7); Rh1 \cdots Rh1, 3.921(4).

Compound **6** has a similar solid state structure to **3** with the phenyl substituent positioned out of the RhP_2 plane and no strong agostic interactions with the vacant site (shortest Rh–C distance greater than 3.3 \AA) making it formally a 16 electron Rh(III) complex.

Table 1: Crystallographic data

Compound	1	2	3	6
CCDC No.	945335	945336	945337	945334
Formula	C ₄₉ H ₆₀ B ₁ Cl ₈ P ₂ Rh ₁	C ₄₂ H ₅₂ B ₁ Cl ₈ P ₂ Rh ₁	C ₈₄ H ₁₀₄ B ₂ Cl ₂ P ₄ Rh ₂ ·3.1(CH ₂ Cl ₂)	0.5(C ₁₁₂ H ₁₁₄ B ₂ Br ₂ F ₄₈ P ₄ Rh ₂)·1.44(CH ₂ Cl ₂)
<i>M</i>	1108.30	1016.16	2295.84	1537.98
Crystal System	Triclinic	Triclinic	Triclinic	Triclinic
Space group	<i>P</i> -1	<i>P</i> -1	<i>P</i> -1	<i>P</i> -1
<i>T</i> [K]	150(2)	150(2)	150(2)	150(2)
<i>a</i> [Å]	12.0494(3)	12.6148(3)	13.2301(3)	13.4344(4)
<i>b</i> [Å]	12.4222(3)	12.7474(3)	17.4742(5)	16.2486(5)
<i>c</i> [Å]	17.4694(4)	16.1361(3)	23.2939(5)	16.3500(5)
<i>α</i> [deg]	88.3937(9)	101.9704(18)	78.048(2)	73.8487(16)
<i>β</i> [deg]	89.8872(9)	102.9988(19)	88.4952(19)	88.5368(15)
<i>γ</i> [deg]	86.3926(9)	106.980(2)	77.569(2)	87.5505(11)
<i>V</i> [Å ³]	2608.61(11)	2311.91(10)	5144.0(2)	3424.70(18)
<i>Z</i>	2	2	2	2
Density [gcm ⁻³]	1.411	1.460	1.482	1.491
<i>μ</i> (mm ⁻¹)	0.831	8.117	8.813	1.068
<i>θ</i> range [deg]	5.10 ≤ <i>θ</i> ≤ 27.47	3.79 ≤ <i>θ</i> ≤ 76.31	3.42 ≤ <i>θ</i> ≤ 76.67	5.120 ≤ <i>θ</i> ≤ 27.507
Reflns collected	20032	23606	54944	27223
<i>R</i> _{int}	0.038	0.027	0.028	0.066
Completeness	98.8 %	98.5 %	98.5%	98.8 %
No. of data/restr/param	10747 / 1312 / 650	9509 / 108 / 523	21268 / 170 / 1110	10296 / 569 / 886
<i>R</i> ₁ [<i>I</i> > 2σ(<i>I</i>)]	0.0628	0.0386	0.0524	0.0606
<i>wR</i> ₂ [all data]	0.1563	0.1050	0.1381	0.1498
<i>GoF</i>	1.0090	1.0037	0.9822	0.9485
Largest diff. pk and hole [eÅ ⁻³]	1.34, -1.29	2.06, -0.80	3.17, -1.75	0.91, -1.08

References

1. A. B. Pangborn, M. A. Giardello, R. H. Grubbs, R. K. Rosen and F. J. Timmers, *Organometallics*, 1996, **15**, 1518-1520.
2. W. E. Buschmann, J. S. Miller, K. Bowman-James and C. N. Miller, *Inorg. Synth.*, 2002, **33**, 83-85.
3. R. Anulewicz-Ostrowska, T. Klis, D. Krajewski, B. Lewandowski and J. Serwatowski, *Tetrahedron Lett.*, 2003, **44**, 7329-7331.
4. G. Giordano and R. H. Crabtree, *Inorg. Synth.*, 1990, **28**, 88-90.
5. A. T. Lubben, J. S. McIndoe and A. S. Weller, *Organometallics*, 2008, **27**, 3303-3306.
6. S. D. Pike, A. L. Thompson, A. s. G. Algarra, D. C. Apperley, S. A. Macgregor and A. S. Weller, *Science*.
7. A. B. Chaplin and A. S. Weller, *Eur. J. Inorg. Chem.*, 5124-5128.
8. J. Cosier and A. M. Glazer, *J. App. Cryst.*, 1986, **19**, 105-107.
9. Z. Otwinowski and W. Minor, in *Macromolecular Crystallography, Pt A*, 1997, vol. 276, pp. 307-326.
10. M. C. Burla, R. Caliandro, M. Camalli, B. Carrozzini, G. L. Casciarano, L. De Caro, C. Giacovazzo, G. Polidori and R. Spagna, *J. App. Cryst.*, 2005, **38**, 381-388.
11. P. W. Betteridge, J. R. Carruthers, R. I. Cooper, K. Prout and D. J. Watkin, *J. Appl. Crystallogr.*, 2003, **36**, 1487.
12. *Crysalis Pro.*, (2011) Oxford Diffraction Ltd, Abingdon, England.
13. L. Palatinus and G. Chapuis, *J. Appl. Crystallogr.*, 2007, **40**, 786-790.
14. P. Vandersluis and A. L. Spek, *Acta Crystallogr. Sect. A*, 1990, **46**, 194-201.
15. A. Spek, *J. Appl. Crystallogr.*, 2003, **36**, 7-13.